American Journal of Pathology, Vol. 159, No. 6, December 2001

Effects of Paramyxoviral Infection on Airway Epithelial Cell Foxj1 Expression, Ciliogenesis, and Mucociliary Function

Dwight C. Look,* Michael J. Walter,* Michael R. Williamson,* Liyi Pang,* Yingjian You,* J. Nicholas Sreshta,* Joyce E. Johnson,† Dani S. Zander,‡ and Steven L. Brody*

From the Department of Internal Medicine, Washington University School of Medicine, St. Louis, Missouri; the Department of Pathology,† Vanderbilt University, Nashville, Tennessee; and the Department of Pathology, Immunology, and Laboratory Medicine,‡ University of Florida College of Medicine, Gainesville, Florida*

To elucidate molecular mechanisms underlying the association between respiratory viral infection and predisposition to subsequent bacterial infection, we used *in vivo* and *in vitro* models and human samples to characterize respiratory virus-induced changes in airway epithelial cell morphology, gene expression, and mucociliary function. Mouse paramyxoviral bronchitis resulted in airway epithelial cell infection and a distinct pattern of epithelial cell morphology changes and altered expression of the differentiation markers β-tubulin-IV, Clara cell secretory protein, and Foxj1. Furthermore, changes in gene expression were recapitulated using an *in vitro* epithelial cell culture system and progressed independent of the host inflammatory response. Restoration of mature airway epithelium occurred in a pattern similar to epithelial cell differentiation and ciliogenesis in embryonic lung development characterized by sequential proliferation of undifferentiated cells, basal body production, Foxj1 expression, and β-tubulin-IV expression. The effects of virus-induced alterations in morphology and gene expression on epithelial cell function were illustrated by decreased airway mucociliary velocity and impaired bacterial clearance. Similar changes in epithelial cell Foxj1 expression were also observed in human paramyxoviral respiratory infection. Taken together, these model systems of paramyxoviral respiratory infection mimic human pathology and identify epithelial cell Foxj1 expression as an early marker of epithelial cell differentiation, recovery, and function. *(Am J Pathol 2001, 159:2055–2069)*

Epithelial cells lining the airways of the lung are constantly subjected to environmental toxins and pathogens. In defense of the lung, an array of innate molecules including chemokines, cytokines, adhesion molecules, and antibacterial proteins are expressed or released by epithelial or immune cells to inactivate the offending agent.[1–3] In addition, a complex mucociliary apparatus constantly clears the airways of organisms and debris.[4] When injured by cytotoxic effects of agents or the inflammatory response, repair mechanisms renew the epithelium to restore these defense systems.[5,6] Despite these mechanisms, respiratory viruses often overcome airway defenses, resulting in significant morbidity and mortality in all age groups.[7,8] Respiratory viruses are the most common cause of airway infection and typically target airway epithelial cells in the upper and lower tract producing airway inflammation and epithelial cell injury. Viral infection also promotes secondary bacterial infection, possibly through injury of epithelial cells, induction of bacteria adherence receptors, and exacerbation of underlying airways diseases.[8–10] Bacterial infection after viral infection is particularly problematic in individuals with acquired (eg, cigarette smokers) or genetic (eg, cystic fibrosis or primary ciliary dyskinesia) epithelial cell abnormalities.[8,9,11] However, healthy children and adults may also develop secondary airway infections,[9,12,13] suggesting a virus-induced failure of normal epithelial cell functions critical for host defense.

Of viruses infecting the human airway, influenza and respiratory syncytial virus (RSV) result in the highest morbidity and mortality.[8,9,14] RSV commonly causes symptomatic infection during early childhood but is increasingly recognized as an important cause of respiratory infection in the elderly.[8,14] A predisposition to bacterial infection with *Hemophilus influenzae*, *Streptococcus pneumoniae*, or *Staphylococcus aureus* has been documented after RSV or influenza infections.[9,12,13] Information regarding airway epithelial injury induced by respiratory viruses has been derived primarily from study of experi-

Supported by awards from the National Institutes of Health (to D. C. L., M. J. W., and S. L. B.), the Cystic Fibrosis Foundation (to D. C. L.), and the American Lung Association (to D. C. L. and M. J. W.)

Accepted for publication August 15, 2001.

Address reprint requests to Steven L. Brody, M.D., Washington University School of Medicine, Campus Box 8052, 660 South Euclid Ave., St. Louis, MO 63110-1093. E-mail: brodys@msnotes.wustl.edu.

mental infections in domestic animals and rodents showing that paramyxovirus (eg, parainfluenza and RSV) infection results in loss of cilia and ciliated cells, hyperplasia of Clara (nonciliated) cells, and, in some animals, secondary bacterial pneumonia.[15–18] Marked cilia loss was also seen after experimental influenza infection of mice and guinea pigs.[19,20] In humans infected with RSV and other respiratory viruses, loss of epithelial cell differentiation and hyperplasia has similarly been described.[21] However, little is known about mechanisms of virus-associated epithelial cell alteration, changes in epithelial cell molecular markers, and the relationship of epithelial cell gene expression to disease pathogenesis.

Recently, identification of transcription factors and other molecular markers expressed in epithelial cells during lung development has helped to elucidate fundamental mechanisms of airway epithelial cell differentiation. The transcription factors Foxa2 (HNF-3β), TTF-1, and GATA-6 are expressed in all epithelial cells beginning at the earliest stages of lung development, persist in the adult airway, and directly regulate expression of lung-specific surfactant proteins and Clara cell secretory protein (CCSP, CC-10).[22–25] Forkhead transcription factor Foxj1 (HFH-4), expressed later during epithelial cell differentiation, is also important in maintenance of airway epithelial cell differentiation through regulation of ciliogenesis.[26–28] The pathological changes in airway epithelial cells during respiratory virus infection suggest that molecular factors controlling differentiation may also be altered. Accordingly, we hypothesized that viral infection alters epithelial cell differentiation resulting in changes in airway epithelial cell-specific gene expression, impaired epithelial cell defense functions, and predisposition to acute bacterial infections.

To assess viral effects on epithelial cells, we induced an inflammatory bronchitis in mice using Sendai Virus (SdV), a paramyxovirus closely related to RSV but pneumotropic for rodents.[29] In this model, we found that cilia and ciliated cells were highly susceptible to direct paramyxovirus injury and that this injury was associated with decreases in Foxj1 expression, the ciliated cell phenotype, and mucociliary clearance. Epithelial repair marked by epithelial cell proliferation, ciliogenesis, and Foxj1 expression occurs before normalization of mucociliary function. Evaluation of human infection with RSV also demonstrated loss of Foxj1 expression, possibly contributing to high morbidity and mortality seen in this viral illness and supporting an important role for Foxj1 in maintenance of epithelial cell function.

Materials and Methods

Mouse Infection with SdV

C57BL/6J mice (6 to 8 weeks old) (Jackson Laboratory, Bar Harbor, ME) were maintained in a biohazard barrier facility in microisolator cages. After anesthesia (80 mg/kg ketamine and 16 mg/kg xylazine, intraperitoneally), mice underwent intranasal administration of a 5×10^3 50% egg infectious dose (EID_{50}) of SdV strain 52 (American Type Culture Collection, Manassas, VA) diluted in 30 μl of sterile phosphate-buffered saline (PBS) as described previously.[29] Control mice were handled identically to virus-inoculated mice but were administered UV-inactivated SdV, 30 μl of PBS, or no treatment. SdV was inactivated by exposure to UV light (Stratolinker 1800; Stratagene, La Jolla, CA) for 6 minutes at 4°C at a total output of 1800 mJ/cm^2. UV-treated SdV was verified nonreplicative in infectivity assays using LLCMK cells as previously described.[30] Mice were weighed daily and examined to monitor for illness and epithelial cell phenotype and airway function were studied at days 3, 5, 8, 12, and 21 after viral inoculation. Sentinel (specific pathogen-free ICN strain) and control mice exhibited no serological or histological evidence of exposure to 11 rodent pathogens, including SdV.

Immunohistochemisty

For lung tissue immunohistochemistry, the trachea was cannulated with a 22-gauge catheter, the lung was inflated under 25-cm H_2O pressure, and the tracheobronchial tree and lungs fixed with 10% buffered formalin for 18 hours or 4% paraformaldehyde for 1 hour at 4°C. When protein expression in trachea was specifically evaluated, the trachea was dissected from the lungs before bronchial cannulation to avoid artifact from the catheter. Paraffin-embedded 6-μm sections were deparaffinized in a D-limonene-based clearing solution (Stephens Scientific, Riverdale, NJ) and rehydrated in graded ethanol solutions. Sections stained with hematoxylin and eosin were used to assess cell morphology. Antigen retrieval was performed by placing slides containing the sections in a citrate-based antigen-unmasking solution (Vector Laboratories, Burlingame, CA) and boiling in a microwave oven as described previously.[27] For peroxidase-based antibody detection, endogenous peroxidase was inactivated by incubation in 3% H_2O_2 in PBS for 5 minutes at 25°C. Nonspecific antibody binding was blocked using 2% fish gel (Sigma-Aldrich, St. Louis, MO) or 2% goat serum in PBS for 30 minutes at 25°C. The samples were then incubated for 18 hours at 4°C with isotype-matched control antibody or primary antibody in blocking solution. Primary antibody binding was detected using a biotinylated secondary antibody with avidin-biotin complex linked to peroxidase (ABC Elite, Vector Laboratories) and 3,3′-diaminobenzidine (DAB) substrate. For SdV antibody detection, avidin-biotin complex linked to alkaline phosphatase was reacted with Vector Red substrate (Vector Laboratories). After immunostaining, sections were counterstained with hematoxylin. For immunofluorescent localization, donkey anti-mouse fluorescein isothiocyanate (FITC)-labeled secondary antibody (1:200; Jackson ImmunoResearch Laboratories, West Grove, PA) was used. Photomicroscopy was performed using a Zeiss Model D-7082 microscope (Carl Zeiss, Thornwood, NY) to acquire electronically digitized images with a charge-coupled device camera (SPOT-2; Diagnostic Instruments, Sterling Heights, MI) interfaced with Spot II software. Primary antibodies (and dilutions used) includ-

ed: biotinylated rat anti-SdV (1:750; BioReliance, Rockville, MD); polyclonal rabbit anti-rat Foxj1 (1:500, generated as previously described[27]); monoclonal mouse anti-human β-tubulin-IV (1:250; BioGenex, San Ramon, CA); polyclonal rabbit anti-mouse Clara cell secretory protein (1:2000; kindly provided by F. DeMayo, Baylor College of Medicine, Houston, TX); polyclonal rabbit anti-rat TTF-1 (1:500; Biopat, Caserta, Italy); polyclonal goat anti-mouse HNF-3β (1:500; Santa Cruz Biotechnology, Santa Cruz, CA); mouse anti-RSV (1:20; Argene, Massapequa, NY); and goat anti-RSV (1:100; Biodesign, Kennebunk, ME).

Electron Microscopy (EM)

Tracheas for scanning and transmission EM were fixed with 2.5% glutaraldehyde in 0.1 mol/L of sodium cacodylate for 1 hour at 4°C, washed, and then incubated with 1.25% osmium tetroxide in PBS for 90 minutes at 25°C. For scanning EM, tracheas were dehydrated in graded baths to 100% ethanol, critical point-dried under liquid carbon dioxide, gold sputter coated, and visualized on a Hitachi S-450 microscope (Hitachi, Tokyo, Japan). For transmission EM, osmium-stained samples were further fixed in 4% uranyl acetate, thin sectioned (90 nm) in Polybed 812 (Polysciences, Warrington, PA), poststained in uranyl acetate and lead citrate, and visualized on a Zeiss 902 microscope.

RNA Blot Analysis

Lung tissue was processed for RNA isolation by flushing the pulmonary vasculature of blood via the right heart with cold 0.1% diethyl pyrocarbonate-treated PBS, freezing in liquid nitrogen, and pulverizing with mortar and pestle. Total cellular RNA was isolated from powdered lung tissues or rat tracheal epithelial (RTE) cell cultures using a combination of guanidinium isothiocyanate lysis and phenol-chloroform extraction (STAT-60; Tel-Test, Friendwood, TX) followed by ethanol precipitation. RNA (5 to 20 μg/sample) was separated by electrophoresis and transferred to charged nylon membranes (Hybond-N, Amersham Pharmacia, Little Chalfont, UK). Probes were labeled with [α-^{32}P] dCTP (>3000 Ci/mmol) by the random-primer technique (Rediprime; Amersham Pharmacia Biotech, International). Probes included the 1.2-kb 3′ cDNA *Eco*RI-*Hin*dIII fragment of mouse Foxj1[31] and the 0.55-kb *Xba*I-*Hin*dIII fragment from pHcGAP containing human glyceraldehyde-3-phosphate dehydrogenase (GAPDH) cDNA in pBR322 (American Type Culture Collection). Hybridization occurred at 42°C for 18 hours and was detected by exposure of membranes to film (Hyperfilm MP, Amersham Pharmacia Biotech) for 1 to 5 days. Foxj1 mRNA levels were normalized to GAPDH mRNA levels using densitometry (Gel Doc 1000; Bio-Rad, Hercules, CA) of radiographs.

RTE Cell Isolation and Culture

RTE cells were harvested and grown on collagen-coated membranes at air-liquid interface using previously reported protocols with minor modifications.[32,33] RTE cells were isolated from adult male Sprague-Dawley rats by incubation of tracheas with 1.5 mg/ml of pronase (Roche Molecular Biochemicals, Indianapolis, IN) overnight at 4°C. Cells were released by agitation and then incubated with 0.5 mg/ml of DNase I for 5 minutes at 4°C. Fibroblasts were removed by adherence on plastic tissue-culture plates (Primera; Becton Dickinson Labware, Franklin Lakes, NJ) for 2 hours at 37°C. Nonadherent epithelial cells were counted and found to have >90% viability when determined by exclusion of trypan blue. RTE cells were resuspended in a defined media consisting of Dulbecco's modified Eagle's media/Ham's F12 (1:1 ratio) supplemented (all from Sigma-Aldrich) with 6.5 mmol/L of L-glutamine, 11.3 mmol/L $NaHCO_3$, 10 μg/ml insulin, 0.1 μg/ml hydrocortisone, 5 μg/ml transferrin, 50 μmol/L phosphoethanolamine, 80 μmol/L ethanolamine, 0.1 μg/ml cholera toxin, 0.03 mg/ml bovine pituitary extract, 30 mmol/L *N*-(2-hydroxyethyl) piperazine-*N*′-2-ethanesulfonic acid (HEPES), 0.5 mg/ml bovine serum albumin, 0.05 μmol/L retinoic acid, 50 U/ml penicillin, 50 μg/ml streptomycin, and 0.25 μg/ml fungizone. A concentration of 10 ng/ml of epidermal growth factor (Becton Dickinson, Bedford, MA) was found to maximize the number of ciliated cells. Cells were seeded at a density of 5×10^5 cells/cm^2 onto 0.33-cm^2 polyester (0.4 μmol/L pore size) membranes (Transwell or Transwell Clear; Corning-Costar, Corning, NY) coated with 50 μg/ml of rat tail collagen (Becton Dickinson) and incubated at 37°C supplemented with 5% CO_2. Nuserum (10%, Becton Dickinson) was added during the first 2 days. Cells were maintained with media in the upper and lower chambers until transmembrane resistance as measured by an epithelial ohmvoltmeter (EVOM; World Precision Instruments, Sarasota, FL) was >300 Ω/cm^2, indicating tight junction formation. Media was then removed from the upper chamber (typically at days 2 to 4) and cells were maintained at air-liquid interface by supplying media daily only to the lower chamber for 2 to 3 weeks to achieve a fully differentiated epithelium. Cells on membranes were monitored by inverted phase microscopy to visualize ciliary activity and estimate the number of ciliated cells. The presence of differentiated, multilayered epithelial cell populations was assessed by scanning EM and histology of sections from paraffin-embedded membranes.

RTE Cell Infection with SdV

Cultured RTE cells were infected with SdV using 2×10^3 EID_{50} in 30 μl of RTE media applied to the apical compartment of 0.33-cm^2 wells containing $\sim 5 \times 10^5$ cells. Cells were incubated with SdV for 24 hours, washed with PBS, and then provided fresh media daily. As a control, parallel wells were treated with UV-inactivated virus of the same titer in an identical manner. After virus infection, cells were harvested by treatment with 150 μl of Cell Dissociation Solution (Sigma) containing 2.5 mg/ml trypsin and 2.7 mmol/L ethylenediaminetetraacetic acid for 30 minutes at 37°C and counted using a hemocytometer. For analysis of protein expression, harvested cells were

washed and transferred to glass slides by cytocentrifugation at 500 rpm for 5 minutes. Alternatively, membranes were fixed with 4% paraformaldehyde for 1 hour at 25°C, washed, and dehydrated in alcohol. To prepare paraffin-embedded cell sections, membranes retained in the Transwell plastic rings were supported by adding 2% agarose in PBS to the underside and, when solidified, to the top of the membrane. The membrane sandwiched within agarose was released from the support with a scalpel blade and embedded in paraffin for sectioning and immunohistochemistry.

Epithelial Cell Proliferation Analysis

Airway epithelial cell density on the mucosal surface of mouse tracheas was determined from low-power magnification scanning EM photomicrographs. Mean cell density for each time point was determined by counting cells within at least five different 10^4-μm^2 areas. To directly analyze cell proliferation, mice were administered 100 mg/kg 5-bromo-2′-deoxyuridine (BrdU) (Sigma-Aldrich) intraperitoneally 20 hours before euthanasia. Lungs were inflated and fixed with 1% paraformaldehyde for 1 hour at 4°C, washed with PBS, and dehydrated in 70% ethanol before paraffin embedding. Tissue sections (6 μm) were deparaffinized, hydrated, and pretreated with blocking solution (Mouse-on-mouse, Vector) to decrease nonspecific antibody binding. A biotinylated monoclonal mouse anti-BrdU antibody (Zymed, South San Francisco, CA) was used according to the manufacturer's protocol and detected using a streptavidin-peroxidase-conjugated secondary antibody and DAB substrate (Zymed). Sections were counterstained with hematoxylin. Foxj1 expression was co-localized with BrdU expression by sequential application of antibodies after sections underwent antigen retrieval by boiling in citrate and denaturing with 2 N HCl for 30 minutes at 37°C. After Foxj1 antibody incubation for 18 hours at 4°C and detection with secondary Cy3-labeled donkey anti-rabbit antibody (Jackson ImmunoResearch Laboratories), the sample was blocked with a BrdU-blocking solution (Zymed), incubated with biotinylated anti-BrdU antibody for 18 hours at 4°C followed by incubation with FITC-labeled avidin (Jackson ImmunoResearch Laboratories). Foxa2 expression was co-localized with BrdU using an identical protocol, except the HCl treatment was omitted and Foxa2 primary antibody was used. A BrdU-labeling index was calculated for airways with epithelial cells incorporating BrdU by counting the number of BrdU expressing nuclei relative to the total number of epithelial cells within 50 to 75 cell regions of airways. A total of 200 to 500 cells were analyzed in each lung section.

Bacterial Clearance Assay

Mice were challenged with aerated, log-phase cultures of nontypable *H. influenzae* strain 12 using a modification of a previously described protocol.[3] Colonies from a fresh plate of *H. influenzae* grown on chocolate blood agar supplemented with 1% Isovitalex were inoculated into 3 to 20 ml of brain-heart infusion broth supplemented with haemin and nicotinamide adenine dinucleotide (NAD). The culture was incubated with rotary shaking at 37°C until a turbidimetric estimate (OD_{600} = 0.7 to 0.8) of 1 to 3×10^9 CFU/ml was achieved (1.5 to 2 hours). Bacteria were then suspended in infection buffer (100 mmol/L NaCl, 10 mmol/L KCl, 10 mmol/L sodium phosphate, pH 7.4, 10 mmol/L glucose, 2% casamino acids) at a concentration of 3×10^6 CFU/ml. Mice were anesthetized with ketamine and xylazine, placed in an intubation apparatus, and orotracheally intubated with a 22-gauge intravenous catheter. A 30-μl volume of bacteria (1×10^5 CFU), was spontaneously inhaled into the airway through the endotracheal catheter, and the mice were allowed to recover. After 16 hours, mice were anesthetized and then euthanized by cervical dislocation. The lungs were exposed, and the pulmonary vascular system was flushed via the right ventricle with sterile saline. Lung tissue was minced in 0.5 ml of PBS and homogenized using a glass tissue grinder. Serial dilutions were inoculated onto solid agar media for culture and quantitation of recovered bacteria. In each assay, animal and lung size varied by <20%, therefore results are expressed as CFU/lung. To quantify leukocyte recruitment into the airway after *H. influenzae* challenge, mice underwent bronchoalveolar lavage and recovered cells were analyzed as previously described.[29]

Mucociliary Velocity Measurements

The movement of particles in the tracheas of anesthetized mice was determined as a measure of mucociliary function using a modification of a previously described method.[34] A narrow anterior window was created in the trachea to visualize the mucosal surface of the trachea. The mouse was positioned under a stereomicroscope at a 20° incline to elevate the head above the body. Polystyrene 0.22-μm beads (FluoSpheres; Molecular Probes, Eugene, Oregon) in 5 μl of PBS were applied to the posterior mucosal surface of the distal tracheal. The cephalad movement of beads was measured throughout time using a ruled grid placed parallel to the trachea. The mean of at least five independent measurements was recorded for each animal.

RSV-Infected Human Samples

Paraffin blocks of lung samples from individuals infected with RSV were obtained from clinical materials collected for routine diagnosis or at autopsy at the University of Vanderbilt Medical Center (Nashville, TN) and the University of Florida Hospital (Gainesville, FL). The use of human samples was approved by the Institutional Review Board of each institution. Samples were analyzed before evaluation in this study by the clinical laboratories at each institution and revealed immunodetectable RSV protein in lung tissues and/or culture of RSV from airway samples.

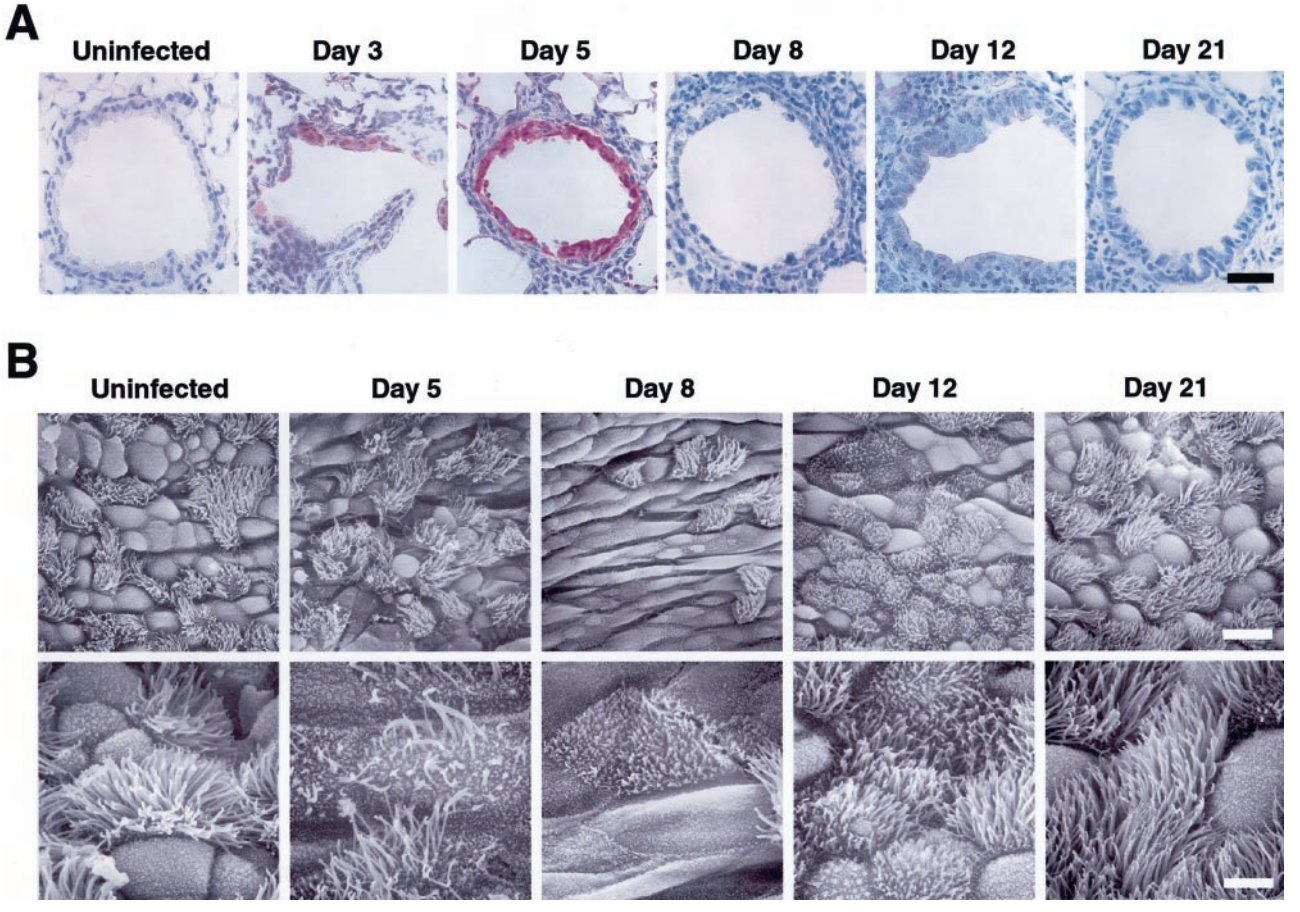

Figure 1. Respiratory paramyxoviral infection alters airway epithelial cell morphology and cilia. Wild-type C57BL/6J mice underwent intranasal inoculation with 5×10^3 EID_{50} of SdV. At the indicated times after inoculation, lungs were harvested for evaluation. **A:** Lungs were subjected to histopathological study in which 6-μm sections were immunostained for SdV protein and detected using alkaline phosphatase and a red chromagen. Representative sections are shown and no detectable staining was observed for nonimmune IgG. Scale bar, 20 μm. **B:** Tracheas were examined by scanning EM at low magnification (**top row**; scale bar, 12 μm), and high magnification (**bottom row**; scale bar, 4 μm).

Statistical Analysis

Cell number, cell antigen expression, bacterial clearance, and mucociliary velocity were analyzed for statistical significance using a one-way analysis of variance for a factorial experimental design. The multicomparison significance level for the one-way analysis of variance was 0.05. If significance was achieved by one-way analysis, postanalysis of variance comparison of means was performed using Scheffé *F*-tests.[35]

Results

Respiratory Paramyxoviral Infection Alters Airway Epithelial Cell Morphology and Cilia

To investigate the impact of viral infection on morphology and differentiation of airway epithelial cells, we used a mouse model of SdV-induced inflammatory tracheobronchitis and bronchiolitis. Uninfected mice were compared to mice administered 5×10^3 EID_{50} of SdV by intranasal application.[29] SdV proteins were detectable in some epithelial cells at day 3, in the majority of epithelial cells throughout the airways (trachea, bronchi, and bronchioles) at day 5, but were no longer detectable by day 8 (Figure 1A) as reported previously.[29] Viral protein expression was detected in both ciliated and nonciliated epithelial cells as previously described[18] and was associated with perivascular and subepithelial inflammation that peaked by day 8 and resolved by day 21.[29] The localization of SdV to epithelial cells and previous reports of changes in cell morphology after respiratory virus infection suggested that paramyxovirus infection could alter airway epithelial cell differentiation.

To initially characterize the alteration in airway epithelial cell phenotype, the luminal surface of the trachea was visualized by scanning EM before and after SdV inoculation. Compared to uninfected animals, mice administered SdV had marked changes in the appearance of nonciliated and ciliated cells (Figure 1B). At day 5, cells were flattened and elongated, cilia were fragmented, and the total number of ciliated cells decreased. At day 8, cells were spindle-shaped and most cilia were absent or shortened. By day 12, recovery of cell morphology was evident by the presence of rounder and smaller cells, an increase in the number of ciliated cells, and cilia lengthening. By day 21, airway epithelial cells appeared similar to controls. Taken together, loss of normal epithelial cell

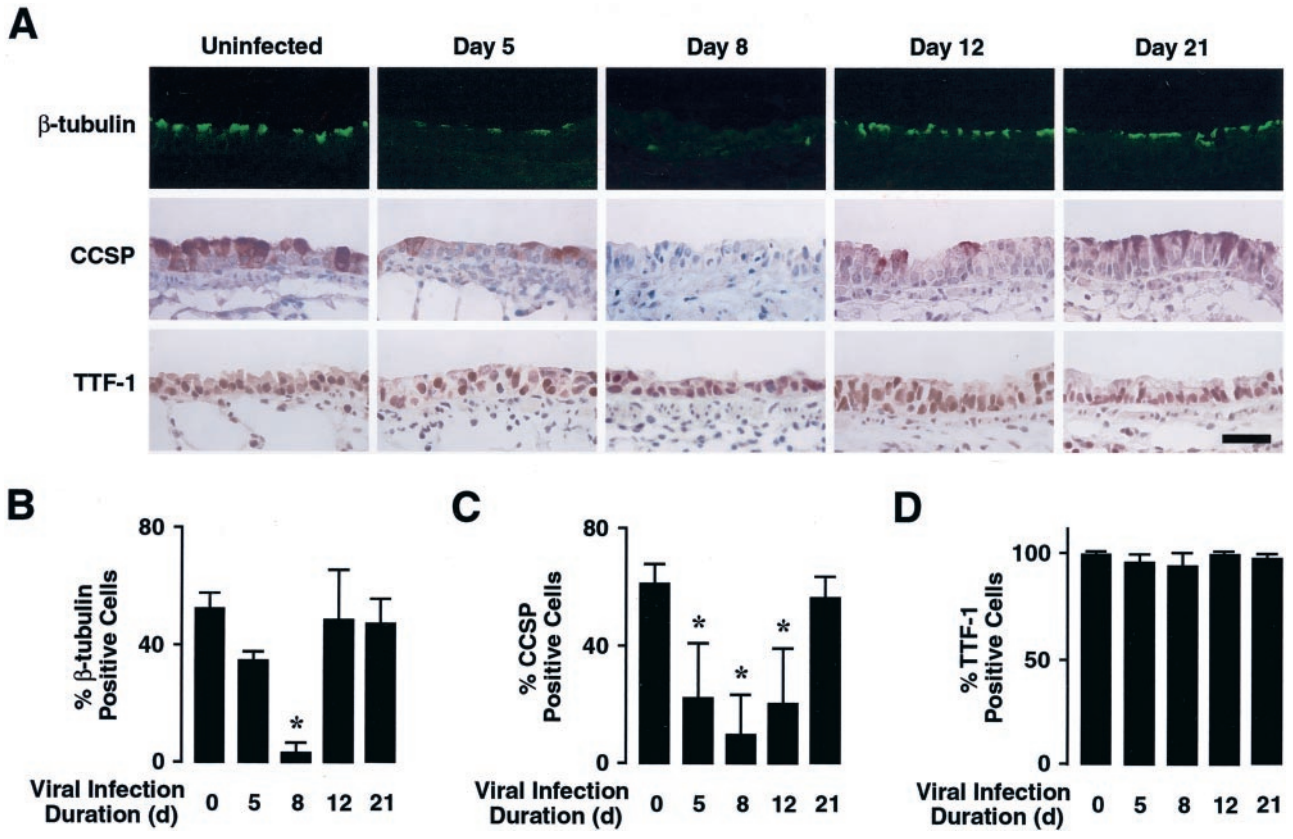

Figure 2. Respiratory paramyxoviral infection alters expression of airway epithelial cell differentiation markers *in vivo*. **A:** Mice underwent intranasal inoculation with SdV as in Figure 1A. At the indicated times after inoculation, lungs were harvested for histopathological study in which 6-μm sections were immunostained for β-tubulin-IV using green FITC fluorescence or for CCSP or TTF-1 using horseradish peroxidase with DAB resulting in a brown product. Representative sections are shown and no detectable staining was observed for nonimmune IgG. Scale bar, 30 μm. The percentage of airway lumen cells that expressed β-tubulin-IV (**B**), CCSP (**C**), and TTF-1 (**D**) were calculated visually using samples from **A**. Values are expressed as mean ± SD (n = 3 to 10 regions from three to five different animals in each group), and a significant decrease compared to mice not infected with SdV is indicated by an **asterisk**.

morphology coincident with or closely after the presence of virus suggested an injury phase, whereas recovery of normal morphology after clearance of virus demarcated a repair phase.

Respiratory Paramyxoviral Infection Alters Expression of Airway Epithelial Cell Differentiation Markers in Vivo

To evaluate alterations in morphology, the expression of molecular markers of differentiation in epithelial cells was assessed. Epithelial cells were initially evaluated for expression of cilia-specific protein β-tubulin-IV, nonciliated cell protein CCSP, and airway epithelial cell protein TTF-1.[25,28] In trachea, bronchi, and bronchioles of uninfected mice, β-tubulin-IV was expressed in ~52.5% of epithelial cells and CCSP in 68.2% of cells (Figure 2; A, B, and C). Although we could not detect cells that expressed both β-tubulin-IV and CCSP, intense and widespread cytoplasmic CCSP expression in tissue sections resulted in overlap of CCSP with other cells and an apparent overestimate of CCSP cell numbers. Despite this phenomenon, throughout a 3-week period after SdV inoculation, there was a period of loss followed by re-expression of these cell proteins, coinciding with phases of injury and repair. Close inspection and cell enumeration indicated that the temporal dynamics of expression of β-tubulin-IV and CCSP differed (Figure 2, B and C). β-tubulin-IV expression was decreased by day 5 and detectable in only a few cells at day 8, but then returned to near normal levels by day 12 (Figure 2B). In contrast, CCSP expression was absent in many airways at days 5 and 8, remained markedly depressed at day 12, and then returned to control levels by day 21 (Figure 2C). Throughout the study period, all cells continued to express TTF-1 (Figure 2D), indicating persistent respiratory epithelial cell gene expression and presence of at least one factor required to support CCSP expression.[23,24] These observations demonstrate that during the course of paramyxoviral infection there is a characteristic loss of markers of cell differentiation suggesting that factors regulating cell differentiation may be absent during the injury and repair phases of infection.

Respiratory Paramyxoviral Infection Causes Loss of Foxj1 Expression in Vivo

The loss of ciliated cells and β-tubulin-IV expression observed at day 8, and return of β-tubulin-IV and the ciliated cell population by day 12, provided a model for

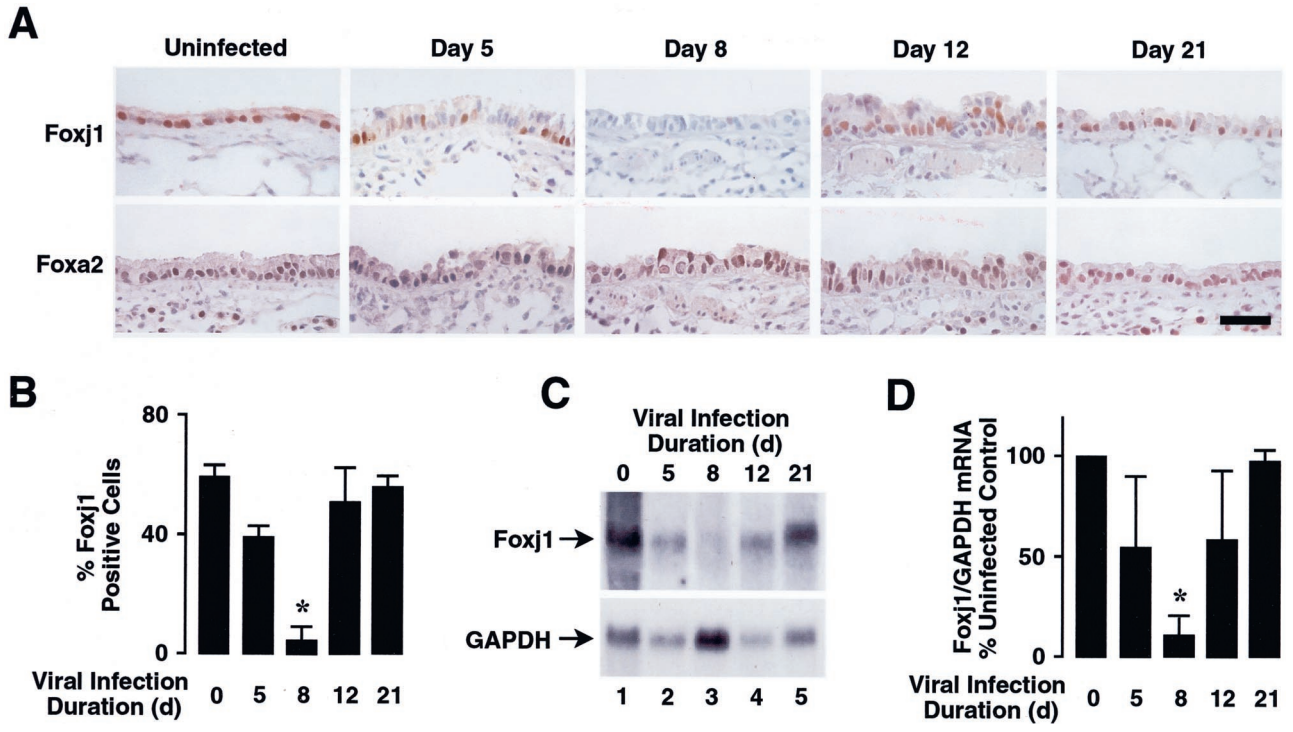

Figure 3. Respiratory paramyxoviral infection causes loss of Foxj1 expression *in vivo*. **A:** Mice underwent intranasal inoculation with SdV as in Figure 1A. At the indicated times after inoculation, lungs were harvested for histopathological study in which 6-μm sections were immunostained for Foxj1 or Foxa2 using horseradish peroxidase and DAB resulting in a brown product. Representative sections are shown and no detectable staining was observed for nonimmune IgG. Scale bar, 30 μm. **B:** The percentage of airway lumen cells that expressed Foxj1 was calculated visually using samples from **A**. Values are expressed as mean ± SD (n = 8 regions from four different animals in each group), and a significant decrease compared to animals not infected with SdV is indicated by an **asterisk**. **C:** Mice were infected with SdV as in Figure 1A. After the indicated durations of infection, total cellular RNA was isolated from lungs. Levels of Foxj1 and GAPDH mRNA were determined by RNA blot analysis and the position of the 1.4-kb Foxj1 and 1.3-kb GAPDH mRNAs are indicated by **arrows**. **D:** Relative levels of Foxj1 mRNA were calculated by densitometry similar to **C**. Values are expressed as mean percent Foxj1/GAPDH RNA level compared to animals not infected with SdV ± SD (n = 3 different animals in each group), and a significant decrease compared to uninfected animals is indicated by an **asterisk**.

assessing regulation of ciliated cell differentiation. The expression of forkhead transcription factor Foxj1 precedes β-tubulin-IV expression and cilia appearance during lung development and is required for airway epithelial cell ciliogenesis.[27,28] Thus, we evaluated expression of Foxj1 in airway epithelial cells after SdV inoculation. Foxj1 was expressed in ~55.7% of airway epithelial cells of uninfected animals, but decreased by day 5 of infection, was detected in few cells at day 8, and recovered by day 12 (Figure 3, A and B). Changes in Foxj1 expression were similar in large and small airways (data not shown). In contrast, expression of forkhead protein Foxa2 (HNF-3β), another marker of airway epithelial cells,[22,25] persisted in the vast majority of airway epithelial cells (Figure 3A). Analysis of total RNA from whole lung of SdV-inoculated mice showed changes in Foxj1 mRNA corresponding to variations in protein expression detected by immunohistochemistry (Figure 3C). This pattern of expression was similar in all mice during the study period when differences in Foxj1 expression were normalized to GAPDH expression (Figure 3D). The observed fall in Foxj1 expression during the injury phase may have been secondary to loss of Foxj1 expression in ciliated cells or death and desquamation of ciliated cells.

Respiratory Paramyxoviral Infection Directly Injures Airway Epithelial Cells with Loss of Foxj1 Expression in Vitro

To assess the direct effect of virus infection on epithelial cell phenotype and to evaluate Foxj1 expression relative to cell loss, RTE cells were infected with SdV using an *in vitro* system for differentiated culture. Observation by phase microscopy after *in vitro* SdV inoculation revealed ciliostasis at day 2 and no beating ciliated cells by day 4 (data not shown). SdV proteins were undetectable in control cells, but after virus inoculation were present in 51 to 74% of epithelial cells (Figure 4, A and B). Uninfected, *in vitro*-differentiated RTE cells visualized by scanning EM appeared similar to epithelial cells in normal rat tracheas with a significant proportion of ciliated surface cells (Figure 4, A and B). On day 2 after SdV inoculation, the number of cilia on cells decreased and cells appeared flattened, but the cell layer remained confluent and there was no significant decrement in cell number from day 0 ($5.58 \times 10^5 \pm 0.34 \times 10^5$ cells) to day 2 ($5.53 \times 10^5 \pm 1.43 \times 10^5$ cells). By day 5, there was a loss epithelial cells ($4.29 \times 10^5 \pm 0.7 \times 10^5$ cells), and remaining cells had infrequent cilia and were flattened and elongated. By day 8, many cells lifted off the membrane typically in cell

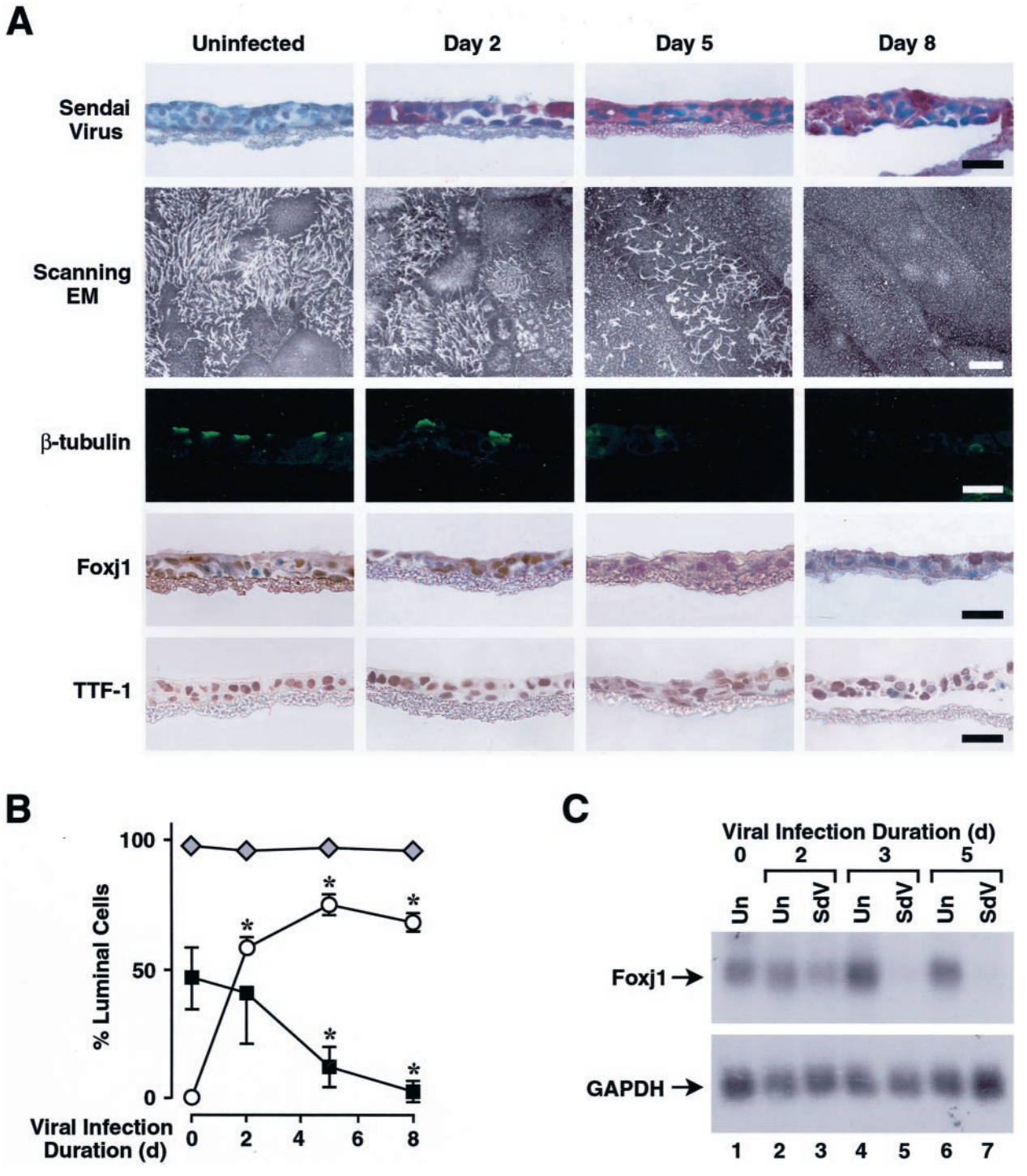

Figure 4. Respiratory paramyxoviral infection directly injures airway epithelial cells with loss of Foxj1 expression *in vitro.* Differentiated RTE cells grown on semipermeable supports under air liquid interface conditions were inoculated with 2×10^3 EID_{50} of SdV. At the indicated times after inoculation, RTE cell were evaluated for gene expressions and changes in morphology. **A:** RTE cells on membrane supports embedded in paraffin were subjected to histopathological study in which 6-μm sections were immunostained for SdV protein and detected using alkaline phosphatase and a red chromagen. Scale bar, 30 μm. RTE cells grown on semipermeable supports were fixed and examined *en face* by scanning EM. Scale bar, 4 μm. RTE cells in sections (as in **A**) were immunostained for β-tubulin-IV using green FITC fluorescence or Foxj1 and TTF-1 using a horseradish peroxidase-DAB resulting in a brown product. Representative sections are shown and no detectable staining was observed for nonimmune IgG. Scale bar, 30 μm. **B:** The percentage of airway cells expressing SdV proteins (**open circles**) calculated from RTE cell cytospin preparations using immunodetection of SdV as in **A**, the percentage of ciliated RTE cells (**closed squares**) calculated visually from low-power-scanning EM images as in **A**, and TTF-1 (**shaded diamonds**) calculated visually using samples from **A**. Values are expressed as mean ± SD (n = 3 to 6 regions from two to three different animals in each group), and a significant difference compared to animals not infected with SdV is indicated by an **asterisk**. **C:** Total cellular RNA was isolated from RTE cells, uninfected (Un) or inoculated with SdV, and levels of Foxj1 and GAPDH mRNA were determined by RNA blot analysis as in Figure 3C. Representative data of three independent experiments is shown.

sheets. Remaining cells lacked cilia, were large, flattened, and elongated with decreased microvilli. Thus, after SdV inoculation, ciliated cell loss, cilia loss, and change from small rounded to large flattened cells characterized both *in vitro* and *in vivo* epithelial cell models.

To determine whether markers of epithelial cell differentiation in our *in vitro* model were expressed in a pattern similar to our mouse model after SdV infection, we performed immunohistochemical analysis of RTE cells. Epithelial cell expression of β-tubulin-IV was decreased at day 2 and was present in only a few cells at days 5 and 8 after viral inoculation (Figure 4A). A similar decline was seen in Foxj1, and at days 5 and 8 Foxj1 expression could only be detected in rare cells. However, TTF-1 remained expressed in nearly all cells (Figure 4, A and B). RNA blot analysis revealed decreased Foxj1 mRNA expression at day 2 after SdV inoculation and marked decreased expression by day 5 (Figure 4C). The decrease in Foxj1 mRNA at day 2 coincided with loss of cilia and preceded and was not proportionate to the subsequent decrease in total cell number. Although changes in the pattern of epithelial cell differentiation markers were similar *in vitro* and *in vivo* during the injury phase, the *in vitro* system did not demonstrate a repair phase characterized by loss of SdV protein expression and return of Foxj1 protein expression.

Respiratory Paramyxoviral Infection Induces Airway Epithelial Cell Proliferation

Repair of injured epithelium could occur by redifferentiation of existing cells and/or proliferation and maturation of new cells. We first determined airway epithelial cell density after *in vivo* SdV inoculation by enumeration of trachea lumen cells from scanning EM images. This revealed that cell density was decreased by day 5, near normal at day 8, and significantly higher than control cell density at day 12 (Figure 5A). By day 21, airway epithelial cell numbers returned to preinoculation levels. To directly assess epithelial cell proliferation, BrdU incorporation (during a 20-hour period) was evaluated in lung sections. In lungs from uninfected mice, only a rare airway epithelial cell demonstrated BrdU incorporation (Figure 5B). However, the number of BrdU-labeled cells increased at day 5, and many clusters of BrdU-positive cells were observed at days 8 and 12. By day 21, few airway epithelial cells demonstrated BrdU incorporation. Quantification of BrdU incorporation in multiple airways confirmed a pattern of increasing proliferation at days 5, 8, and 12, with return to control levels by day 21 (Figure 5C). Thus, at least one mechanism of epithelium repair is through generation of new cells.

Respiratory Paramyxoviral Infection Leads to an Ordered Epithelial Repair Process

The production of new airway epithelial cells and reappearance of markers of epithelial cell differentiation after viral infection indicated that a program of epithelial cell maturation followed proliferation and recapitulated lung development. The previously established relationship of Foxj1 expression to the ciliated cell phenotype implied that Foxj1 could direct the fate of cell differentiation,[27,36] but the ciliogenesis stage-specific expression of Foxj1 had not been determined. Transmission EM was used to identify cells committed to the ciliated type at an early stage of differentiation by assessing the presence of cilia precursor structures (centrioles or basal bodies) present before generation of axonemes.[37] Transmission EM of tracheas at day 5 after SdV inoculation demonstrated loss of axonemes in cells, but retention of basal bodies that were docked at the apical membrane (Figure 6A). At day 8 (when Foxj1 expression was markedly decreased), axonemes were not present and centrioles and basal bodies were scattered within the cytoplasm. The location of centrioles in epithelial cells at day 8 after viral inoculation was similar to that seen in Foxj1 null mice (Figure 6A) indicating a cell already committed to the ciliated phenotype, but at an early stage of ciliogenesis.[28] In contrast to Foxj1 null mice, the position of basal bodies in epithelial cells at day 8 after viral inoculation was transient because by day 12 (when Foxj1 expression increased) basal bodies were docked at the apical membrane and axoneme growth was occurring. Colocalization studies of BrdU and Foxj1 showed mutually exclusive expression at days 5, 8, and 12 after viral inoculation (Figure 6B, and data not shown) suggesting Foxj1 does not have a role in cell fate determination before or during proliferation and ciliated cells are not progenitors for other ciliated cells after SdV infection. In contrast, all cells that incorporated BrdU also expressed Foxa2 (Figure 6C), suggesting that a relatively undifferentiated cell must commit to become a ciliated cell before regulation by Foxj1.

Respiratory Paramyxoviral Infection Impairs Airway Clearance

To assess the effect of airway virus infection and consequent alterations in epithelial cell morphogenesis and gene expression on airway defense function, mice were administered a sublethal dose of nontypable *H. influenzae* on days 5, 12, or 21 after SdV inoculation. Mice challenged with bacteria at day 5 after SdV inoculation had a 23-fold decrease in *H. influenzae* clearance (Figure 7A). Compared to mice 5 days after SdV infection, bacterial clearance improved in mice 12 days after infection (twofold decreased compared to control), and clearance was similar to that of uninfected mice by day 21. Multiple airway defense mechanisms are required for efficient bacterial clearance in the airway including antibacterial substances, mucus, and immune cells.[1,4] At days 5 and 12, SdV inoculated mice had a twofold increase in airway neutrophils recovered by bronchoalveolar lavage compared to uninfected mice (data not shown), indicating that impaired neutrophil recruitment was not the cause of depressed bacterial clearance. Alternatively, the loss of cilia could be an important factor altering bacterial clearance after paramyxovirus virus injury. In support of this

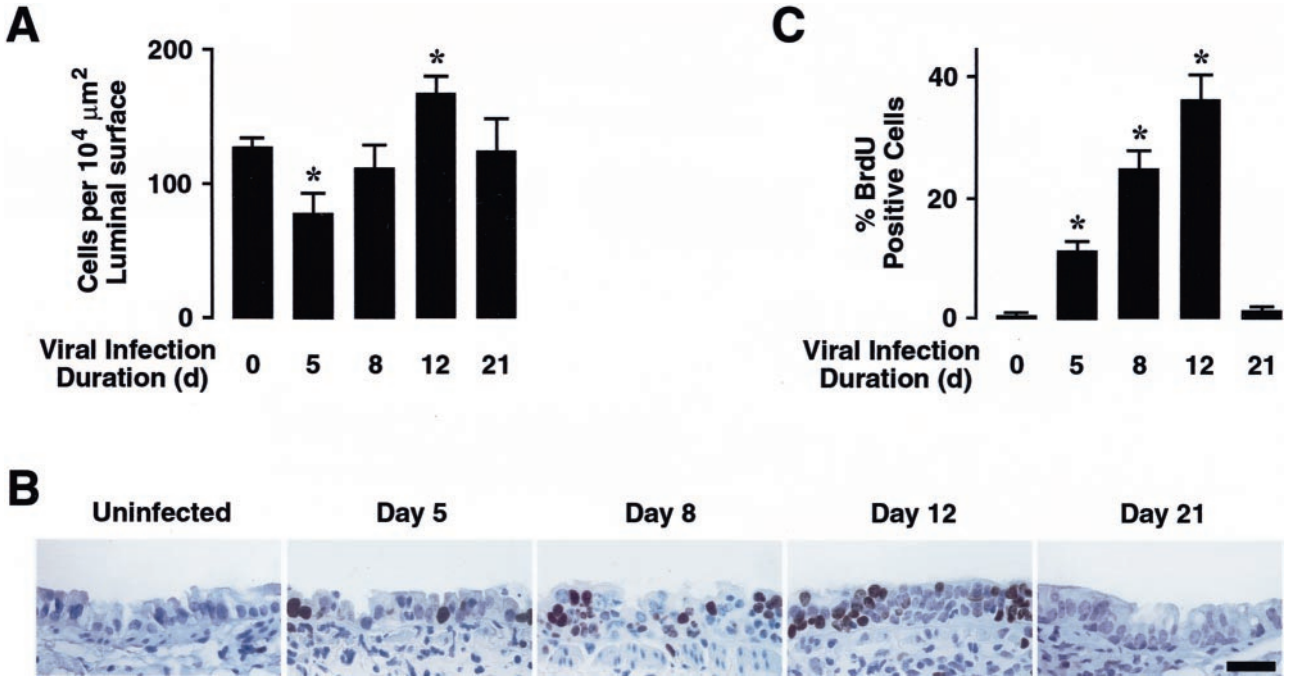

Figure 5. Respiratory paramyxoviral infection induces airway epithelial cell proliferation. **A:** Mice underwent intranasal inoculation with SdV as in Figure 1A. At the indicated times after inoculation, lungs were harvested for examination by scanning EM. Luminal cell density was calculated visually in 10^4-μm^2 areas. Values are expressed as mean ± SD (n = 5 regions from two to three different animals in each group), and a significant difference compared to animals not infected with SdV is indicated by an **asterisk**. **B:** Mice were infected with SdV as in Figure 1A, and 20 hours before evaluation animals were administered intraperitoneal BrdU. After the indicated duration of infection, lungs were harvested for histopathological study in which 6-μm sections were immunostained for BrdU using horseradish peroxidase and DAB to produce a brown product. Samples were counterstained with hematoxylin. Representative sections are shown and no detectable staining was observed for nonimmune IgG. Scale bar, 20 μm. **C:** The percentage of airway lumen cells that expressed BrdU was calculated visually using samples from **B**. Values are expressed as mean ± SD (n = 5 to 11 regions from two to three different animals in each group), and a significant increase compared to animals not infected with SdV is indicated by an **asterisk**.

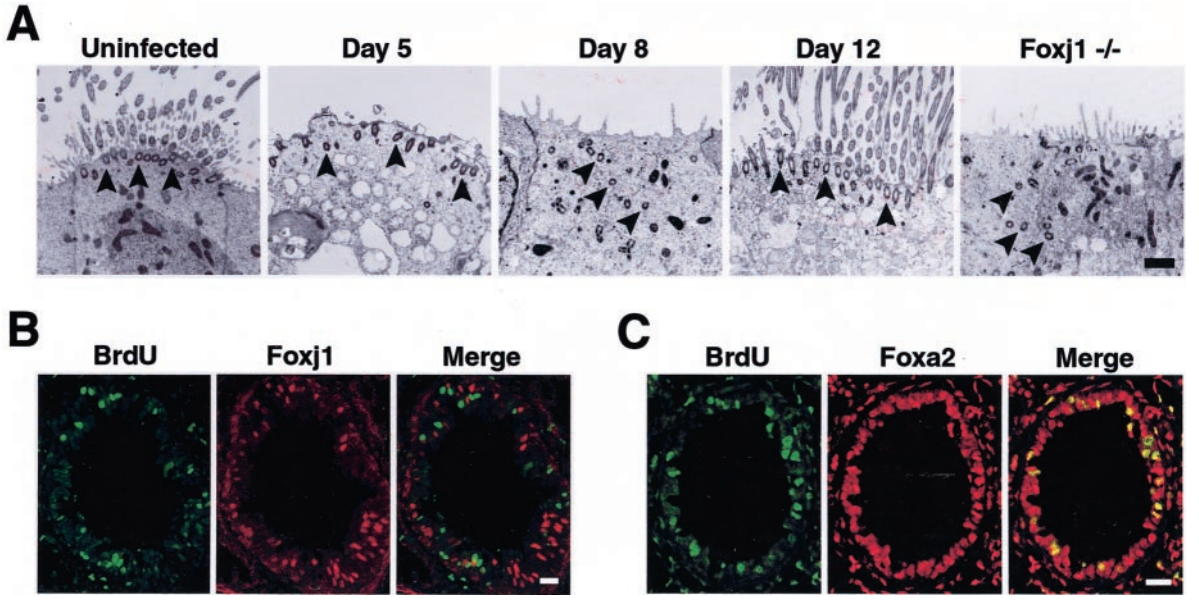

Figure 6. Respiratory paramyxoviral infection leads to an ordered epithelial repair process. **A:** Wild-type C57BL/6J mice underwent intranasal inoculation with SdV as in Figure 1A. At the indicated times after inoculation, lungs were harvested for examination by transmission EM. Shown at the far **right** is a section from an uninfected Foxj1 null (−/−) mouse. **Arrowheads** indicate location of basal bodies. Scale bar, 1 μm. **B:** Mice were infected with SdV as in Figure 1A and administered BrdU as in Figure 5B. After 12 days, lungs were harvested for study in which 6-μm sections were immunostained for BrdU using green FITC fluorescence and Foxj1 using red Cy3 fluorescence. Scale bar, 30 μm. **C:** Samples obtained as described in **B** were immunostained for BrdU using green FITC fluorescence and Foxa2 using red Cy3 fluorescence. Scale bar, 30 μm.

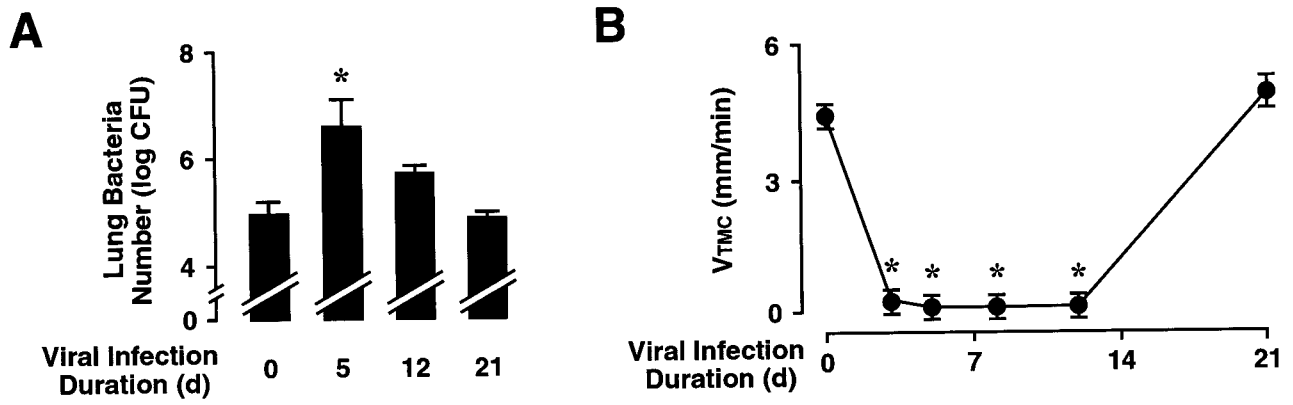

Figure 7. Respiratory paramyxoviral infection impairs airway clearance. **A:** Mice were infected with SdV as in Figure 1A for the indicated durations, followed by tracheobronchial inoculation with 10^5 cfu of nontypable *H. influenzae* strain 12. After 16 hours of bacterial infection, lung homogenates were prepared for quantitation of *H. influenzae*. Values are expressed as mean ± SD (n = 3 to 6 in each group), and a significant increase compared to animals not infected with SdV is indicated by an **asterisk**. **B:** Mice were infected with SdV as in Figure 1A. At the indicated times after inoculation, mice were anesthetized, and the velocity of 0.2-μm polystyrene beads within the trachea was determined. Values are expressed as mean ± SD (n = 3 to 5 in each group), and a significant decrease compared to animals not infected with SdV is indicated by an **asterisk**.

concept, we found that Foxj1 null mice (that lack cilia) inoculated with *H. influenzae* had a 37-fold decrease in bacterial clearance compared to control mice (data not shown). To more directly determine the role of mucociliary function in airway clearance after airway virus infection, the rate of movement of polystyrene beads (a surrogate for infectious particles and airway debris) on the mucosal layer of the mouse trachea was measured after SdV inoculation. A significant decrease in the ability of the mucociliary apparatus to move beads was noted at 5, 8, and 12 days after virus inoculation (Figure 7B). Bead velocity returned to baseline levels by day 21. These results correlated with studies in Foxj1 null mice that had no detectable bead movement (<1 mm/minute; data not shown). Thus, changes in mucociliary velocity provide one potential mechanism for the decrease in bacterial clearance seen in mice after SdV inoculation.

Human Respiratory Paramyxoviral Infection Results in Loss of Foxj1 Expression

Having found that paramyxovirus infection in mice was associated with marked alteration in epithelial cell phenotype, we sought to determine whether a similar phenomenon occurred in humans infected with paramyxovirus. Accordingly, we evaluated the expression of airway epithelial cell differentiation markers in lung samples from individuals infected with RSV (Table 1). Lung from the control patient demonstrated a pattern of Foxj1 and TTF-1 expression similar to uninfected mice with all airway epithelial cells expressing TTF-1 and ~60% expressing Foxj1 (Figure 8). As observed in mouse airways after SdV infection, TTF-1 expression persisted in airway epithelial cells of patients infected with RSV. Notably, airway epithelial cells in serial sections from RSV-infected patient showed decreased or absent expression of Foxj1. The length of respiratory signs and symptoms (possibly indicating the duration of infection) in patients varied, as did morphological changes in airway epithelial cells. Some samples showed more extensive epithelial cell loss (patients 3 and 5) and/or airways filled with debris including desquamated clumps of bronchial epithelial and inflammatory cells (patient 4). However, virus-induced changes in airway epithelial cell gene expression observed in our mouse model were also found in human paramyxovirus infection, suggesting that the molecular program regulating cell differentiation during injury and repair is conserved. In addition, some patients acquired secondary bacterial pneumonia consistent with previous reports identifying this clinical association[9] and with virus-associated defect in airway clearance that we observed in SdV-infected mice. The loss of ciliogenesis factor Foxj1 in both mouse models and human infection associated with significant morbidity and mortality emphasizes the importance of this protein as a marker in injury, repair, and function of ciliated epithelial cells in the airway.

Table 1. Patients with RSV Infection Analyzed for Foxj1 Expression

Sample	Age	Gender	Underlying diseases	Duration of symptoms*	Outcome
Control	60 years	Male	Pneumonectomy for adenocarcinoma	—	—
Patient 1	64 years	Female	Lung transplant, diabetes mellitus	1 day	Survived
Patient 2	15 months	Male	Congenital heart disease	2 days	Bacterial pneumonia, died
Patient 3	2 months	Male	Recurrent apnea, sepsis	5 days	Bacterial pneumonia, died
Patient 4	77 years	Male	Chronic lymphocytic leukemia	7 days	Bacterial pneumonia, died
Patient 5	63 years	Male	Non-Hodgkin's lymphoma	16 days	Died

*Before obtaining lung tissue.

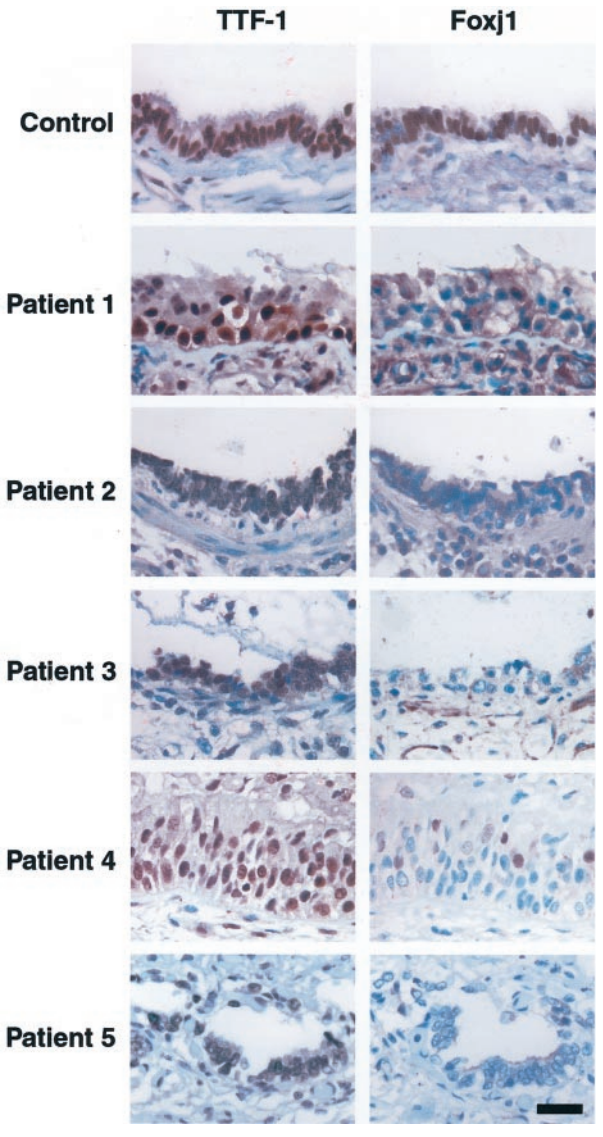

Figure 8. Human respiratory paramyxoviral infection causes loss of Foxj1 expression. Samples from lungs obtained during diagnostic or postmortem examination of patients uninfected (control) or infected with RSV (patients 1 to 5) as demonstrated by immunostaining and or sample culture. Serial 6-μm sections were immunostained for Foxj1 and TTF-1 and detected using horseradish peroxidase and DAB to produce a brown product. Samples were counterstained with hematoxylin. Representative sections are shown and no detectable staining was observed for nonimmune IgG. Scale bar, 20 μm.

Discussion

The association of serial changes in airway epithelial cell morphology with molecular markers of differentiation after respiratory virus infection have not been described previously nor correlated with measures of mucociliary function. However, the clinical relationship between respiratory virus infection and secondary bacteria pneumonia is well known[9,12,13] and has been postulated to be related to changes in epithelial cell phenotype.[9] Using rodent experimental models and human tissues obtained after respiratory paramyxovirus infection, we observed that changes in airway epithelial cells segregated into two distinct phases: an injury phase, characterized by loss of cilia, decreased expression of markers of cell differentiation, and depressed mucociliary function; followed by a repair phase identified by epithelial cell proliferation, subsequent expression of molecular markers of differentiation, ciliogenesis, and recovery of mucociliary function. Paramyxovirus-induced loss of cilia during the injury phase led us to focus on forkhead transcription factor Foxj1 because it is required for normal ciliogenesis during lung development.[28] The loss of Foxj1 expression and other molecular markers of differentiation in SdV-infected mice was associated with impaired mucociliary function quantified by assays of bacterial clearance and mucociliary velocity. The relevance of these findings to human disease is demonstrated by decreased Foxj1 expression and secondary bacteria infection in patients with RSV infection, suggesting that altered cell phenotype has important implications in human paramyxovirus infection. Although recovery from respiratory virus infection could not be monitored by serial biopsy from patients, our mouse model revealed an ordered process of proliferation and differentiation, with expression of molecular markers in a pattern that mirrored lung development. Thus, these findings link epithelial cell injury and altered differentiation with defects in host defense, providing mechanisms for secondary bacterial infections in human paramyxovirus and related respiratory virus infections.

The spectrum of morphological changes that we observed in airway epithelial cells are consistent with reports in other animal species infected with paramyxoviruses and other viruses.[15–20] Epithelial cell flattening, hyperplasia, and cilia loss have been observed in experimental animals and humans after respiratory infection with different serotypes of paramyxoviruses and influenza virus.[15,16,20,21,38] *Ex vivo* influenza A infection of isolated piglet trachea and *in vitro* RSV infection of primary human bronchial epithelial cell cultures have also shown marked loss of cilia and ciliated cells suggesting a direct virus effect.[39,40] Influenza A virus infection has been shown to result in loss of ciliated cells and decreased mucociliary clearance in the eustachian tube of guinea pigs, a structure that shares features with the lower airway.[41] The specific mechanisms for morphological changes affecting ciliated and nonciliated cells have not been identified, but tropism of viruses for airway epithelial cells may lead to shared responses in the targeted cells of the respiratory tract.

The specific molecular responses and epithelial cell phenotypic changes that we observed were associated with virus infection and several potential direct and indirect mechanisms may lead to altered gene expression. One mechanism that likely accounts for morphological changes in the airway epithelium is virus-induced epithelial cell cytotoxicity and loss that may be characteristic of SdV infection and other viruses.[42] This virus-induced injury may be related, at least in part, to innate and adaptive immune responses generated by the infection.[43–46] However, the similarity of cell injury that we observed *in vivo* and *in vitro* suggested that viruses per se induce characteristic injury and morphological changes independent of immune cells. In addition, we observed changes in cell morphology and gene expression out of proportion to cell infection, suggesting that the morphol-

ogy of uninfected cells may be altered through other mechanisms. The flattened and elongated changes observed in airway epithelial cells by scanning EM *in vivo* and *in vitro* may be the result of uninfected cells extending to cover denuded basement membrane, as seen in airway wound models.[5,6,47] It is also possible that changes in epithelial cell phenotype are a response to cytokines such as interferon-α/β, interferon-γ, interleukin-1β, or interleukin-8 that are released after virus infection.[2,40,48] Epithelial cell differentiation can also be altered by growth factors, hormones, and retinoic acid[32] that could be affected by viral infection. *In vitro*, these factors were provided in media that was replaced daily, but it is possible that infected cells have altered receptors and/or signaling, or cell products are released that interrupt biochemical pathways of cell differentiation. It is also possible that alterations in differentiation are a stereotypical response to epithelial cell injury alone and not specific to respiratory viral injury. However, we have found that mice exposed to cigarette smoke also have injury and loss of airway epithelial cell cilia, but Foxj1 expression remains unaffected (Dwight C. Look, Michael R .Williamson, Steven L. Brody, unpublished observation). In any event, it is currently unknown if specific respiratory viral proteins can directly interfere with differentiation pathways.

After injury and before restoration of normal epithelial cell differentiation, cell proliferation and sequential induction of Foxj1, β-tubulin-IV, and CCSP were observed. Cell proliferation is central to repair of epithelium in other injury models[5,6] and it is unclear if injured cells can redifferentiate after virus injury. Cell proliferation is reflected as cell hyperplasia found in lung samples after virus infection in experimental animal models[16,17] and after human respiratory virus infections.[21] Interestingly, we found that at day 12 after *in vivo* SdV inoculation, the number of airway epithelial cells seems to have increased above the normal level, as an overshoot, but returning to normal levels by day 21 (Figure 5A). The mechanism of this overshoot of epithelial cell proliferation is unclear and other studies will need to be done to confirm this finding and elucidate mechanisms of airway repair.

To follow epithelial cell differentiation during the repair phase of viral infection, we used molecular markers previously characterized during epithelial cell differentiation in the developing lung. Throughout injury and repair phases of infection, there was persistent expression of Foxa2 and TTF-1. These proteins are fundamental markers of airway epithelial cells expressed early in the differentiation program.[22,23,25] The lack of Foxj1 and CCSP expression reflects epithelial cells at a relatively undifferentiated (but not necessarily pleuripotent) state of development. Persistent Foxa2 and TTF-1 expression during virus-induced injury may be because of a relative resistance of some cell populations to SdV infection[18] and suggest that early programs of epithelial cell differentiation remain intact. An absence of CCSP in epithelial cells throughout the airways suggests that it is unlikely that mature Clara cells are functioning as a reservoir for new differentiated cells after viral infection. However, the current lack of early Clara cell markers makes it difficult to completely exclude this source of a progenitor or stem cell population. When cells do differentiate during the repair phase after virus injury, the lag of CCSP expression relative to the appearance of β-tubulin-IV and Foxj1 could be explained by a requirement for programs of differentiation that are identical to lung development. In the developing mouse lung, the onset of expression of Foxj1 is embryonic day 15, β-tubulin-IV approximately embryonic day 16, and CCSP embryonic day 17, suggesting airway repair recapitulates development.[25,27]

Because of the importance of Foxj1 in ciliogenesis, we focused on the role of Foxj1 during cilia loss and repair after viral infection. In SdV injury models, Foxj1 expression correlated with the presence or absence of ciliated cells. The decrease in number of cilia after virus infection could be because of impaired ciliogenesis (because of a direct effect of SdV on Foxj1 expression), direct cilia loss (because of virus toxicity), or ciliated cell death. The role for Foxj1 in the repair process is consistent with its critical role in ciliogenesis during lung development. Our previous observations showed a cilogenesis defect in the Foxj1 null mouse,[28] and epithelium repair after virus injury provided another model to investigate the expression of Foxj1 during different stages of ciliogenesis. After SdV injury, ultrastructural changes in basal body localization in new (or differentiating) epithelial cells corresponded with changes in Foxj1 expression. These observations suggested a role for Foxj1 in determining the ciliated cell phenotype (ie, immediately after proliferation) or directing maturation of these cells (ie, late after proliferation and centrilogenesis). Two observations support the proposition that Foxj1 likely does not play an early role in cell phenotype determination. First, Foxj1 expression is markedly depressed at day 8 although at this time we find an abundance of new cells already committed to the ciliated cell phenotype as evidenced by induction of centriologenesis (basal bodies present in the cytoplasm).[37] Second, there is an absence of Foxj1 expression in cells in the proliferative and early postproliferative phases of epithelial repair are marked by BrdU labeling of cells throughout a period of 20 hours. Instead, it is more probable that Foxj1 is important for late-stage ciliogenesis related to basal body positioning at the apical membrane.

In the mouse SdV model, depressed Foxj1 expression throughout a 5- to 10-day period that includes epithelial cell injury and early repair spans a window of ciliated cell deficiency and impaired host defense. The association of loss of Foxj1 and other markers of epithelial cell differentiation with impaired mucociliary function identified factors that may be important in causing the clinical syndrome of postrespiratory virus bacterial pneumonia. Decreased Foxj1 expression in samples obtained from patients with severe RSV infection supported this association. Thus, it was not surprising that some of the individuals with RSV infection that we evaluated developed bacterial pneumonia after RSV infection. Although a direct relationship between virus infection and decreased Foxj1 expression is suggested, the complex nature of illnesses affecting each individual makes it also possible

that changes in differentiation could be the result of underlying diseases or other pathogens. Nonetheless, it is notable that Foxj1 expression was consistently absent in patient samples and that changes in epithelial cells observed in the mouse SdV model were reflected in the human samples. Additionally, changes in epithelial cell differentiation after respiratory virus infection may also explain why individuals with underlying diseases that impair mucociliary function or virus clearance (eg, cigarette smoking, emphysema, or cystic fibrosis) may have increased morbidity and mortality after viral infection compared to a normal host. Thus, rapid re-expression or up-regulation of proteins such as Foxj1 might minimize impaired airway clearance after respiratory virus infection and prevent complications.

Acknowledgments

We thank F. DeMayo (Baylor College of Medicine, Houston, TX) for providing CCSP antibody and M. Veith (Washington University Department of Biology) and L. LaRose (Washington University Department of Cell Biology) for assistance with EM.

References

1. Zhang P, Summer WR, Bagby GJ, Nelson S: Innate immunity and pulmonary host defense. Immunol Rev 2000, 173:39–51
2. Thomas LH, Wickremasinghe MI, Sharland M, Friedland JS: Synergistic upregulation of interleukin-8 secretion from pulmonary epithelial cells by direct and monocyte-dependent effects of respiratory syncytial virus infection. J Virol 2000, 74:8425–8433
3. Frick AG, Joseph TD, Pang L, Rabe AM, St Geme III JW, Look DC: Haemophilus influenzae stimulates ICAM-1 expression on respiratory epithelial cells. J Immunol 2000, 164:4185–4196
4. Wanner A, Salathé M, O'Riordan TG: Mucociliary clearance in the airway. Am J Respir Crit Care Med 1996, 154:1868–1902
5. Erjefalt JS, Erjefalt I, Sundler F, Persson CG: In vivo restitution of airway epithelium. Cell Tissue Res 1995, 281:305–316
6. Kauffman SL: Cell proliferation in the mammalian lung. Int Rev Exp Pathol 1980, 22:131–191
7. Hemming VG: Viral respiratory diseases in children: classification, etiology, epidemiology, and risk factors. J Pediatr 1994, 124:S13–S16
8. Glezen WP, Greenberg SB, Atmar RL, Piedra PA, Couch RB: Impact of respiratory virus infections on persons with chronic underlying conditions. JAMA 2000, 283:499–505
9. Hament JM, Kimpen JL, Fleer A, Wolfs TF: Respiratory viral infection predisposing for bacterial disease: a concise review. FEMS Immunol Med Microbiol 1999, 26:189–195
10. Jiang Z, Nagata N, Molina E, Bakaletz LO, Hawkins H, Patel JA: Fimbria-mediated enhanced attachment of nontypeable Haemophilus influenzae to respiratory syncytial virus-infected respiratory epithelial cells. Infect Immun 1999, 67:187–192
11. Jeffery PK, Brain AP, Shields PA, Quinn BP, Betts T: Response of laryngeal and tracheo-bronchial surface lining to inhaled cigarette smoke in normal and vitamin A-deficient rats: a scanning electron microscopic study. Scanning Microsc 1988, 2:545–552
12. Takala AK, Meurman O, Kleemola M, Kela E, Ronnberg PR, Eskola J, Makela PH: Preceding respiratory infection predisposing for primary and secondary invasive Haemophilus influenzae type b disease. Pediatr Infect Dis J 1993, 12:189–195
13. Kim PE, Musher DM, Glezen WP, Rodriguez-Barradas MC, Nahm WK, Wright CE: Association of invasive pneumococcal disease with season, atmospheric conditions, air pollution, and the isolation of respiratory viruses. Clin Infect Dis 1996, 22:100–106
14. Dowell SF, Anderson LJ, Gary Jr HE, Erdman DD, Plouffe JF, File Jr TM, Marston BJ, Breiman RF: Respiratory syncytial virus is an important cause of community-acquired lower respiratory infection among hospitalized adults. J Infect Dis 1996, 174:456–462
15. Bryson DG, McNulty MS, McCracken RM, Cush PF: Ultrastructural features of experimental parainfluenza type 3 virus pneumonia in calves. J Comp Pathol 1983, 93:397–414
16. Castleman WL, Lay JC, Dubovi EJ, Slauson DO: Experimental bovine respiratory syncytial virus infection in conventional calves: light microscopic lesions, microbiology, and studies on lavaged lung cells. Am J Vet Res 1985, 46:547–553
17. Castleman WL: Alterations in pulmonary ultrastructure and morphometric parameters induced by parainfluenza (Sendai) virus in rats during postnatal growth. Am J Pathol 1984, 114:322–335
18. Massion PP, Funari CC, Ueki I, Ikeda S, McDonald DM, Nadel JA: Parainfluenza (Sendai) virus infects ciliated cells and secretory cells but not basal cells of rat tracheal epithelium. Am J Respir Cell Mol Biol 1993, 9:361–370
19. Ramphal R, Fischlschweiger W, Shands Jr JW, Small Jr PA: Murine influenzal tracheitis: a model for the study of influenza and tracheal epithelial repair. Am Rev Respir Dis 1979, 120:1313–1324
20. Azoulay-Dupuis E, Lambre CR, Soler P, Moreau J, Thibon M: Lung alterations in guinea-pigs infected with influenza virus. J Comp Pathol 1984, 94:273–283
21. Aherne W, Bird T, Court SDM, Gardner PS, McQuillin J: Pathological changes in virus infections of the lower respiratory tract in children. J Clin Pathol 1970, 23:7–18
22. Costa RH, Kalinichenko VV, Lim L: Transcription factors in mouse lung development and function. Am J Physiol 2001, 280:L823–L838
23. Bohinski RJ, Di Lauro R, Whitsett JA: The lung-specific surfactant protein B gene promoter is a target for thyroid transcription factor 1 and hepatocyte nuclear factor 3, indicating common factors for organ-specific gene expression along the foregut axis. Mol Cell Biol 1994, 14:5671–5681
24. Bingle CD, Hackett BP, Moxley M, Longmore W, Gitlin JD: Role of hepatocyte nuclear factor-3α and hepatocyte nuclear factor-3β in Clara cell secretory protein gene expression in the bronchiolar epithelium. Biochem J 1995, 308:197–202
25. Zhou L, Lim L, Costa RH, Whitsett JA: Thyroid transcription factor-1, hepatocyte nuclear factor-3β, surfactant protein B, C, and Clara cell secretory protein in developing mouse lung. J Histochem Cytochem 1996, 44:1183–1193
26. Hackett BP, Brody SL, Liang M, Zeitz ID, Bruns LA, Gitlin JD: Primary structure of hepatocyte nuclear factor/forkhead homologue 4 and characterization of gene expression in the developing respiratory and reproductive epithelium. Proc Natl Acad Sci USA 1995, 92:4249–4253
27. Blatt EN, Yan XH, Wuerffel MK, Hamilos DL, Brody SL: Forkhead transcription factor HFH-4 expression is temporally related to ciliogenesis. Am J Respir Cell Mol Biol 1999, 21:168–176
28. Brody SL, Yan XH, Wuerffel MK, Song SK, Shapiro SD: Ciliogenesis and left-right axis defects in forkhead factor HFH-4-null mice. Am J Respir Cell Mol Biol 2000, 23:45–51
29. Walter M, Kajiwara N, Karanja P, Castro M, Holtzman M: Interleukin 12 p40 production by barrier epithelial cells during airway inflammation. J Exp Med 2001, 193:339–352
30. Kiyotani K, Takao S, Sakaguchi T, Yoshida T: Immediate protection of mice from lethal wild-type Sendai virus (HVJ) infections by a temperature-sensitive mutant, HVJpi, possessing homologous interfering capacity. Virology 1990, 177:65–74
31. Brody SL, Hackett BP, White RA: Structural characterization of the mouse Hfh4 gene, a developmentally regulated forkhead family member. Genomics 1997, 45:509–518
32. Kaartinen L, Nettesheim P, Adler KB, Randell SH: Rat tracheal epithelial cell differentiation in vitro. In Vitro Cell Dev Biol Anim 1993, 29A:481–492
33. Ostrowski LE, Randell SH, Clark AB, Gray TE, Nettesheim P: Ciliogenesis of rat tracheal epithelial cells in vitro. Methods Cell Biol 1995, 47:57–63
34. Zahm JM, Gaillard D, Dupuit F, Hinnrasky J, Porteous D, Dorin JR, Puchelle E: Early alterations in airway mucociliary clearance and inflammation of the lamina propria in CF mice. Am J Physiol 1997, 272:C853–C859
35. Zar JH: Biostatistical Analysis. Englewood Cliffs, Prentice-Hall, 1984
36. Tichelaar JW, Wert SE, Costa RH, Kimura S, Whitsett JA: HNF-3/

forkhead homologue-4 (HFH-4) is expressed in ciliated epithelial cells in the developing mouse lung. J Histochem Cytochem 1999, 47:823–831
37. Sorokin SP: Reconstruction of centriole formation and ciliogenesis in mammalian lungs. J Cell Sci 1968, 3:207–230
38. Noble RL, Lillington GA, Kempson RL: Fatal diffuse influenzal pneumonia: premortem diagnosis by lung biopsy. Chest 1973, 63: 644–646
39. Fishaut M, Schwartzman JD, McIntosh K, Mostow SR: Behavior of respiratory syncytial virus in piglet tracheal organ culture. J Infect Dis 1978, 138:644–649
40. Tristram DA, Hicks Jr W, Hard R: Respiratory syncytial virus and human bronchial epithelium. Arch Otolaryngol Head Neck Surg 1998, 124:777–783
41. Ohashi Y, Nakai Y, Esaki Y, Ohno Y, Sugiura Y, Okamoto H: Influenza A virus-induced otitis media and mucociliary dysfunction in the guinea pig. Acta Otolaryngol 1991, 486(Suppl):S135–S148
42. Heylbroeck C, Balachandran S, Servant MJ, DeLuca C, Barber GN, Lin R, Hiscott J: The IRF-3 transcription factor mediates Sendai virus-induced apoptosis. J Virol 2000, 74:3781–3792
43. Faden H, Hong JJ, Ogra PL: Interaction of polymorphonuclear leukocytes and viruses in humans: adherence of polymorphonuclear leukocytes to respiratory syncytial virus-infected cells. J Virol 1984, 52:16–23
44. Wang SZ, Xu H, Wraith A, Bowden JJ, Alpers JH, Forsyth KD: Neutrophils induce damage to respiratory epithelial cells infected with respiratory syncytial virus. Eur Respir J 1998, 12:612–618
45. Cannon MJ, Openshaw PJ, Askonas BA: Cytotoxic T cells clear virus but augment lung pathology in mice infected with respiratory syncytial virus. J Exp Med 1988, 168:1163–1168
46. Zhao MQ, Stoler MH, Liu AN, Wei B, Soguero C, Hahn YS, Enelow RI: Alveolar epithelial cell chemokine expression triggered by antigen-specific cytolytic CD8(+) T cell recognition. J Clin Invest 2000, 106: R49–R58
47. Dunsmore SE, Saarialho-Kere UK, Roby JD, Wilson CL, Matrisian LM, Welgus HG, Parks WC: Matrilysin expression and function in airway epithelium. J Clin Invest 1998, 102:1321–1331
48. Saunders NA, Smith RJ, Jetten AM: Differential responsiveness of human bronchial epithelial cells, lung carcinoma cells, and bronchial fibroblasts to interferon-γ in vitro. Am J Respir Cell Mol Biol 1994, 11:147–152